Surface & Coatings Technology 258 (2014) 913–920

Contents lists available at ScienceDirect

Surface & Coatings Technology

journal homepage: www.elsevier.com/locate/surfcoat

In vitro cytocompatibility evaluation of hydrogenated and unhydrogenated carbon films

B. Liu, T.F. Zhang, B.J. Wu, Y.X. Leng *, N. Huang

Key Laboratory for Advanced Technologies of Materials, Ministry of Education, School of Materials Science and Engineering, Southwest Jiaotong University, Chengdu, 610031, China

ARTICLE INFO

Article history:
Received 14 March 2014
Accepted in revised form 20 July 2014
Available online 26 July 2014

Keywords:
Hydrogenated amorphous carbon (a-C:H)
Unhydrogenated amorphous carbon (a-C)
Osteoblast
Macrophages
Covalent binding
Unpaired electrons

ABSTRACT

Hydrogenated amorphous carbon (a-C:H) films and unhydrogenated amorphous carbon (a-C) films are promising as artificial joint coatings due to their excellent wear resistance. In this paper, the cytocompatibility of a-C:H film and a-C film was evaluated to determine the more appropriate type for prosthesis modification. The a-C:H film was deposited by electron convolute resonance plasma enhanced chemical vapor deposition (ECR-PECVD) and a-C film was fabricated by magnetic filtered cathodic vacuum arc (MFCVA). The microstructure and physical characteristics of the films were investigated by Raman spectroscopy, contact angle measurement, atom force microscopy (AFM), electrokinetic analysis, electrical resistivity measurement and Hall effect measurement. Bovine serum albumin (BSA) and serum protein adsorption on a-C and a-C:H films was determined by micro BCA assay. RAW264.7 macrophages were cultured on the a-C:H and a-C films for 24 h to evaluate the cell death, cell activation and inflammatory cytokine release. Primary mouse osteoblasts were cultured on the a-C:H and a-C films for 2 h, 1 day, 3 days and 6 days with biological tests performed to evaluate the cell adhesion, cell viability and cell morphology. The results show that a-C film is N type semiconductor with unpaired electrons. Protein adsorption assay shows that the a-C film can covalently bind more serum proteins than a-C:H film. The unpaired electrons of a-C film contribute to its better ability to covalently bind bioactive proteins than a-C:H film, and the superior adsorption and bioactivity of the adhesion proteins on a-C film further induce the better biological performance of a-C film. In a word, a-C film induces lower inflammatory reaction and higher ostoblasts viability than a-C:H film.

1. Introduction

As the most direct and effective treatment of advanced hip joint diseases, for example, traumas, osteoarthritis, rheumatoid arthritis, or bone tumors, artificial hip joints have been successfully applied in clinic and greatly improved the quality of patients' life. The common types of artificial joint are metal-on-polymer (MOP), metal-on-metal (MOM) and ceramic-on-ceramic (COC). The wear rate of the MOM prosthesis, which is made of CoCrMo alloy, is about 0.3 mm^3/year, presenting 1%–2.5% of the wear of traditional MOPs [1,2]. Such good wear resistant makes MOM a promising friction pair. However, CoCr debris and metal ions such as Co^{2+} and Cr^{3+} can be generated due to the wear and corrosion process, which would induce pro-inflammatory response, cytotoxicity to osteoblasts and even DNA damage [3–5]. As a result, there is serious risk of aseptic loosening and genotoxicity with this type of implant, and this restricts the application of MOM in artificial arthroplasty [6]. In 2010, Depuy Orthopaedics Inc recalled all the ASR MOM surface replacement system and ASR™ XL MOM total hip replacement system due to the undesirable response caused by metal debris. Despite all these drawbacks, the unique advantage to form large size femoral head, which offers a greater range of motion, makes the MOM joints desirable and attractive for active patients in younger age. In order to resolve the problems caused by wear debris, methods to reduce the wear of MOM joints have been widely investigated.

Diamond like carbon (DLC) film is deemed to be a promising solution of MOM joints aseptic loosening since DLC coating is hard, wear resistant and chemically inert [7,8]. The wear of DLC-coated CoCrMo–CoCrMo joint is 10^5–10^6 times lower than that of conventional MOM hip joints [9]. In order to further promote the application of DLC films in load bearing joints, the biological properties of DLC films have been wider analyzed in the recent years [10–14]. DLC stands for a group of carbon films, which can be divided into hydrogenated carbon film and unhydrogenated carbon film, namely, a-C:H film and a-C film. It has been proven that both a-C:H and a-C films influence the adhesion and viability of osteoblasts in a positive way and reduce inflammatory reactions compared to Si, polyetheretherketone (PEEK), stainless steel and Silicon nitride (Si_3N_4) ceramics [10–12,14]. The biological property of various DLCs may be different due to different surface energy, surface roughness and microstructure, which are causally determined by the fabrication method and deposition parameters [15–17]. Hence, it is of great significance to find out whether a-C film or a-C:H film has better

* Corresponding author. Tel./fax: +86 28 87601149.
E-mail address: yxleng@263.net (Y.X. Leng).

http://dx.doi.org/10.1016/j.surfcoat.2014.07.059
0257-8972/

biocompatibility and which properties of the DLC films have major impact on the biocompatibility.

In this work, a-C:H film was deposited by electron convolute resonance plasma enhanced chemical vapor deposition (ECR-PECVD) and a-C film was fabricated by magnetic filtered cathodic vacuum arc (MFCVA). The microstructure, surface properties, the inflammation reaction and mouse calvaria osteoblast behavior of the films were evaluated.

2. Materials and methods

2.1. Sample preparation

Mirror polished Co alloy (Cr: 28.02%, Mo: 6.11%, Ni: 0.2%, C: 0.062%, Co: bal) disks (10 mm diameter and 2 mm thickness) were used as a positive control. In order to eliminate adverse effect caused by the metal substrate in biocompatibility evaluation, single-crystal silicon wafer (EMEI Semiconductor, Sichuan, China) was used as the substrate of a-C and a-C:H film. Glass was also used as the substrate for a-C and a-C:H film to conduct electrical property measurement. The a-C film (about 60 nm thick) was prepared by MFCVA as reported by Liu et al. [18] and a-C:H film (about 80 nm thick) was prepared by ECR-PECVD as reported by Deng et al. [19]. The DLC coated Si wafer was then cut into 10 mm × 10 mm square and ultraviolet sterilized (30 min for each side) and then put into 24-well plates before biological testing.

2.2. Surface characterization

Raman spectra from 800 cm^{-1} to 2000 cm^{-1} were obtained using Raman spectrometer (Renishaw Invia, UK) activated by a 514 nm Ar^{+} laser. The wettability of DLC film was characterized by static contact angle measurements using a Drop Shape Analyzer DSA100 (KRÜSS, Germany) with distilled water, diiodomethane and glycerol. Five different areas of the sample were chosen to get representative data. The average value and the standard deviation were used to calculate the surface energy following the Owen–Wendt theory according to the given software. An AFM (CSPM 5000, China) was used to evaluate the surface morphology of DLC films. The root-mean-square roughness (RMS) was obtained by tapping mode. Zeta potential of DLC film was measured by an electro kinetic analyzer (EKA, Anton Paar GmbH, Graz, Austria) in 0.001 M KCl (pH = 7.4 ± 0.3) solution. Ten data of each sample were examined and the average value is reported. Electrical resistivity of a-C film and a-C:H film was detected by a four point probe tester (SZ-82, China). Conductivity type and carrier mobility of DLC films were measured by a Hall effect measurement system (ET-9002, China).

2.3. Protein adsorption

Bovine serum albumin (BSA) and serum protein from culture medium (a-MEM with 5% FBS) were used for protein adsorption assay and protein adsorption was analyzed using the micro BCA protein assay (Thermo Scientific, America). For BSA adsorption, each sample was immersed in 1 ml of BSA (2 mg/ml protein in PBS) solution at 37 °C for 24 h. For serum protein adsorption, each sample was immersed in a 1 ml of culture medium at 37 °C for 2 h. After the incubation, samples were washed three times with PBS to remove the non-adherent proteins. To quantify the covalent bound proteins, additional samples are immersed in culture medium for 2 h and then immersed in 2% sodium dodecyl sulphonate (SDS) for 2 h followed by rinsing in water for 3 times to remove the non-covalently bound proteins. All the samples were blow-dryed, then 150 μl micro bicinchoninic acid (BCA) working reagent was peptted onto each sample in a 24 well plate and incubated at 37 °C for 120 min. At last, 100 μl working reagent was collected and measured at 562 nm.

2.4. Evaluation of inflammatory reaction

Macrophages are commonly used for evaluation of inflammatory reactions, as they are central inflammatory cells, connecting the innate and the adaptive immune system [20]. RAW 264.7 murine macrophages were cultured in Dulbecco's modified Eagle's medium (DMEM, Corning cellgro@, USA) supplemented with 10% fetal bovine serum (FBS). Prior to cell seeding, macrophages were mechanically dispersed and adjusted to 1×10^5 cells/ml with culture medium. Then 1 ml/well cell suspension was added onto the sterilized samples and incubated at 37 °C with 5% CO_2 for 24 h.

2.4.1. Cell death

After incubation for 24 h, macrophage death was investigated immediately by acridine orange and propidium iodide (AO/PI) staining [21]. AO can pass through the intact cell membrane and bind to the nuclear DNA, resulting in bright green fluorescence, but PI can only pass through an impaired cell membrane and binds to the nuclear DNA, leading to orange fluorescence. Stock solutions of AO (100 μg/ml) and PI (100 μg/ml) in phosphate buffered saline (PBS) were mixed with culture medium at the ratio of 1:1:100. The harvested samples were rinsed three times with PBS and transferred into a new 24-well plate. Thereafter, 350 μl staining reagent was added on each sample and later incubated at 37 °C with 5% CO_2 for 5 min. Then the samples were observed by an inverted fluorescence microscope (OLYMPUS IX51, Japan). More than seven random images at the same magnification were obtained for statistically analysis of adherent cells.

2.4.2. Cell morphology

Samples were rinsed three times with PBS, fixed with 2.5% glutaraldehyde overnight at 4 °C and then the fixed samples were again rinsed three times with PBS. Afterwards, samples were dehydrated in a graded ethanol series (50%, 75%, 90%, and 100% vol/vol) for 15 min each and later dealcoholized using isoamyl acetate at the same procedure as for dehydration. After that, samples were put in the fume hood overnight so that isoamyl acetate completely evaporated. The dry specimens were sputter coated with gold before SEM observation. Morphology of the macrophages was acquired by scanning electron microscopy (SEM, Quanta 200, FEI, Holland).

2.4.3. Cytokine analysis

The supernatant of each sample was collected and stored at −20 °C until cytokine analysis. Levels of tumor necrosis factor-α (TNF-α) and interleukin-6 (IL-6) were determined using commercial sandwich enzyme-linked immunosorbent assay (ELISA) kits (Boster, China), following the instructions of the manufacturer.

2.5. Primary mouse osteoblast culture and evaluation

Primary mouse osteoblasts were obtained from mouse calvaria according to standard tissue culture protocols [22]. Osteoblasts were cultured in Minimum Essential Medium Alpha (a-MEM, Corning cellgro@, USA) supplemented with 5% FBS. The osteoblast monolayers were trypsin digested and cells were adjusted to 5×10^4 cells/ml with culture medium, then 1 ml/well cell suspension was seeded onto the samples and incubated at 37 °C with 5% CO_2.

2.5.1. Cell adhesion

After a 2 h incubation, samples were removed and fixed overnight before staining by 4′,6-diamidino-2-phenylindole (DAPI) for cell counting. A fluorescence microscope was used to obtain random 15 images for statistics of attached cell.

2.5.2. Cell viability

The viability of the osteoblasts was investigated using a cell counting kit (CCK-8, Japan) after 1, 3, and 6 days of culture. At each time points,

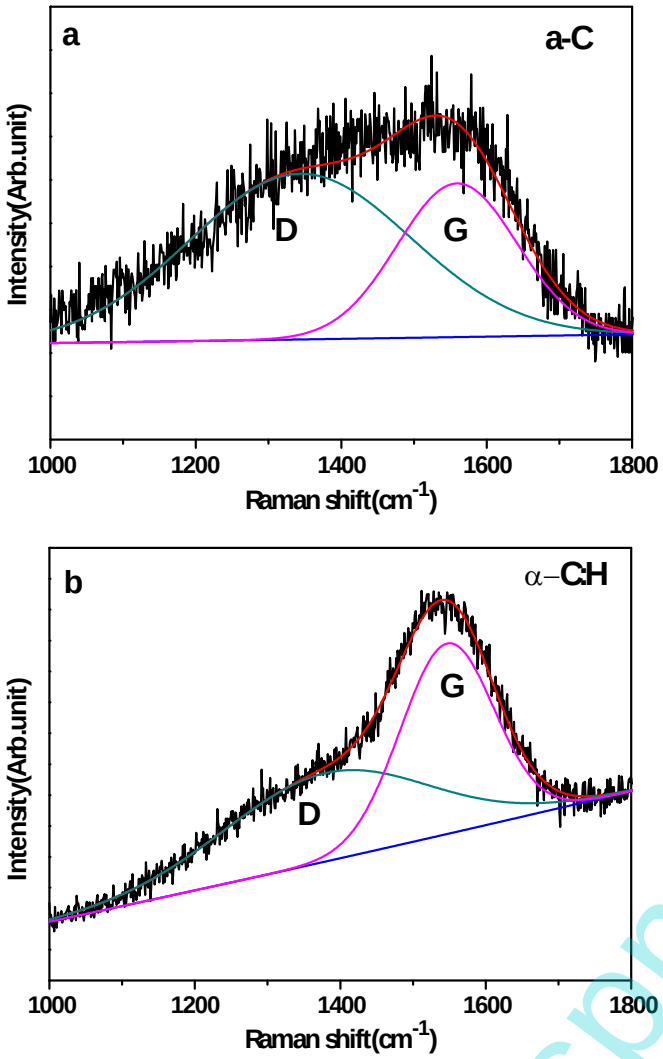

Fig. 1. Gaussian fitted Raman spectrum of a-C film and a-C:H film.

the harvested specimens were transferred into fresh 24-well cell culture plates with 0.35 ml/well fresh culture medium containing 10% CCK-8 solution and then incubated with the samples for 4 h. Finally, 0.2 ml incubated medium was transferred to a 96-well plate for OD measurement at 450 nm.

2.5.3. Cell morphology

Fluorescence microscopy was applied to observe the cell morphology of osteoblasts cultured for 1 day and 3 days by staining with rhodamine 123. The harvested samples were rinsed three times with PBS. Afterwards, 50 μl rhodamine 123 was added to make sure it spread out on the whole surface of each sample. Cell staining was operated in darkroom for 15 min, and the stained samples were again rinsed with PBS three times. Then the samples were blown dry before observation.

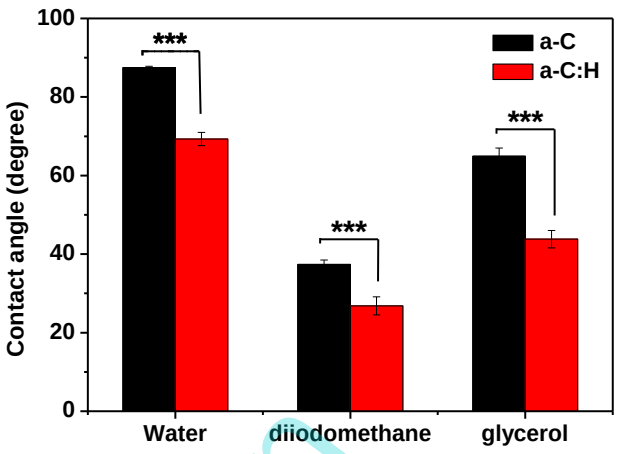

Fig. 2. Contact angles of a-C film and a-C:H film. (Data given as mean ± SD, the statistical significance is indicated by $^{***}p < 0.001$, $n = 5$).

2.6. Statistical analysis

One-way ANOVA was performed using the software SPSS 17 (Chicago, Illinois) to determine statistical differences between the samples. Data are given as mean ± standard deviation (SD). $p < 0.05$ was considered as significant difference.

3. Results

3.1. Material characterization

DLC is a metastable form of amorphous carbon containing both sp^2 (graphite like) bonds and sp^3 (diamond-like) bonds [13]. The microstructure of the DLC films was studied by Raman spectroscopy, and results are shown in Fig. 1. To analyze the structure of a-C film and a-C:H film, the spectra were then processed by linear background subtraction and Gaussian curve fitting with limit of less than 400 cm^{-1} full width at half maximum (FWHM). It is well known that the additional disorder peak at about 1335 cm^{-1} (D band) displays disordered or fine graphite crystallites, while the single sharp peak at about 1580 cm^{-1} (G band) is the presentation of large single-crystal graphite and highly oriented pyrolytic graphite [23]. The relative intensity of the disorder-induced D peak to that of the G peak (I_D/I_G) is related to the graphitic content and sp^3 fraction [23,24]. As shown in Table 1, for a-C film, the D band is at 1343.1 cm^{-1} and G band is at 1559.4 cm^{-1} with I_D/I_G ratio of 1.99. For a-C:H film, the D band is at 1380.0 cm^{-1} and G band is at 1546.7 cm^{-1} with I_D/I_G of 1.01. The larger I_D/I_G ratio of a-C films indicates that a-C films have a higher sp^2 fraction but a lower sp^3 fraction than a-C:H film.

The physical/chemical characterization of a-C film and a-C:H film is summarized in Table 1. The contact angles of a-C film and a-C:H film for water, diiodomethane and glycerol are given in Fig. 2. The water contact angle of the a-C:H film and the a-C film are 69.9 ± 3.2 degrees and 87.5 ± 0.3 degrees, respectively. The a-C:H film shows a slightly more hydrophilic state than a-C film, and the surface energy of the a-C:H film is larger than a-C film (shown in Table 1). The surface morphology of a-C film and a-C:H film was studied by AFM in tapping mode and the

Table 1
Summarized results from physical/chemical characterization of a-C film and a-C:H film.

	D band (cm^{-1})	D-FWHM (cm^{-1})	G band (cm^{-1})	G-FWHM (cm^{-1})	I_D/I_G	Surface energy (mN/m)	RMS (nm)	Electrical resistivity (Ω · cm)
a-C	1343.1	357.7	1559.4	193.5	1.99	36.78	0.363	1.70×10^{-3}
a-C:H	1380.0	328.8	1546.7	150.7	1.01	45.77	1.462	Insulating

Table 2
Result of protein adsorption using micro BCA assay (data given as mean ± SD, the statistical significance is indicated by * $p < 0.05$, $n = 4$).

Protein	Material	
	a-C	a-C:H
BSA ($OD_{562\ nm}$)	0.76 ± 0.15	0.43 ± 0.10
Serum protein ($OD_{562\ nm}$)	0.39 ± 0.05	0.26 ± 0.03
Serum protein (after SDS cleaning, $OD_{562\ nm}$)	0.28 ± 0.07	0.19 ± 0.05

RMS of a-C films and a-C:H films is 0.363 nm and 1.462 nm, respectively (shown in Table 1), representing the ultra-high smooth surface of these two DLC films. The zeta potentials of the a-C film and the a-C:H film were measured by an electro kinetic analyzer in 0.001 M KCl (pH = 7.4 ± 0.3) solution. The zeta potential of a-C and a-C:H is −6.8 ± 0.8 mV and −5.5 ± 1.3 mV, respectively. Electrical resistivity of a-C and a-C:H films was determined by a four point probe tester. The a-C:H film is an insulator while the electrical resistivity of a-C film is $1.7 \times 10^{-3}\ \Omega \cdot cm$. Hall effect measurement shows that a-C film is N type semiconductor and the carrier mobility is 55.0 $cm^2\ V^{-1}\ s^{-1}$, indicating a large amount of unpaired electrons in a-C film. No carrier mobility is detected in a-C:H film.

3.2. Protein adsorption

The protein adhered on the films was determined with a micro BCA assay, and the determined OD values are given in Table 2. Both BSA and serum protein are used in this work, because BSA is commonly used as a model protein and serum protein contains complex proteins that approaches to physiological environment. Results show that a-C film adsorbed more BSA and serum protein than a-C:H film, indicating the better protein adsorption capability of a-C film. From Table 2, it is observed that more serum proteins are remained on a-C film after cleaning with SDS, a detergent capable of disrupting noncovalent interactions, which indicates that a-C film covalent binds more proteins than a-C:H film.

3.3. Inflammation response

The Raw 264.7 macrophage line was used to evaluate the inflammation response to a-C and a-C:H films. Death of macrophages was determined by AO/PI staining, and images are shown in Fig. 3, green cells are vital, orange cells represent dead ones. Most of the macrophages on Co alloy (Fig. 3a) show an orange fluorescence, indicating that many macrophages were activated and then died. Fig. 3b (a-C film) shows that all the cells are green, meaning no macrophage death on a-C. Some cells on the a-C:H film (Fig. 3c) also are orange, but the death rate is lower compared to Co alloy.

Morphology changes of macrophages are related to their immune function [25]. Macrophages normally are round in shape, but once stimulated, they extend pseudopodia to phagocyte the foreign bodies [26]. SEM images of macrophages cultured on Co alloy and DLC films for 24 h re shown in Fig. 4. Fig. 4a shows that the cells on Co alloy are totally spread, occupying a large area, extending a large number of pseudopodia with an extremely irregular shape. This is the typical morphology of activated macrophages [27,28]. Cells on a-C (Fig. 4b) and a-C:H films (Fig. 4c) show less activated morphology. Some macrophages on the a-C surface (Fig. 4b) are spherical with no or few pseudopodia extending, indicating lower inflammation reaction. Macrophages are spherically on a-C:H film as shown in Fig. 4c, but many cells are with multiple pseudopodia. Thus, it can be assumed that a-C induces less activation of the macrophages than a-C:H.

TNF-α and IL-6 are bone-resorbing or osteolytic factors that can be released by activated macrophages [29,30]. In order to further evaluate the inflammatory reaction, the cytokines (IL-6 and TNF-α) were

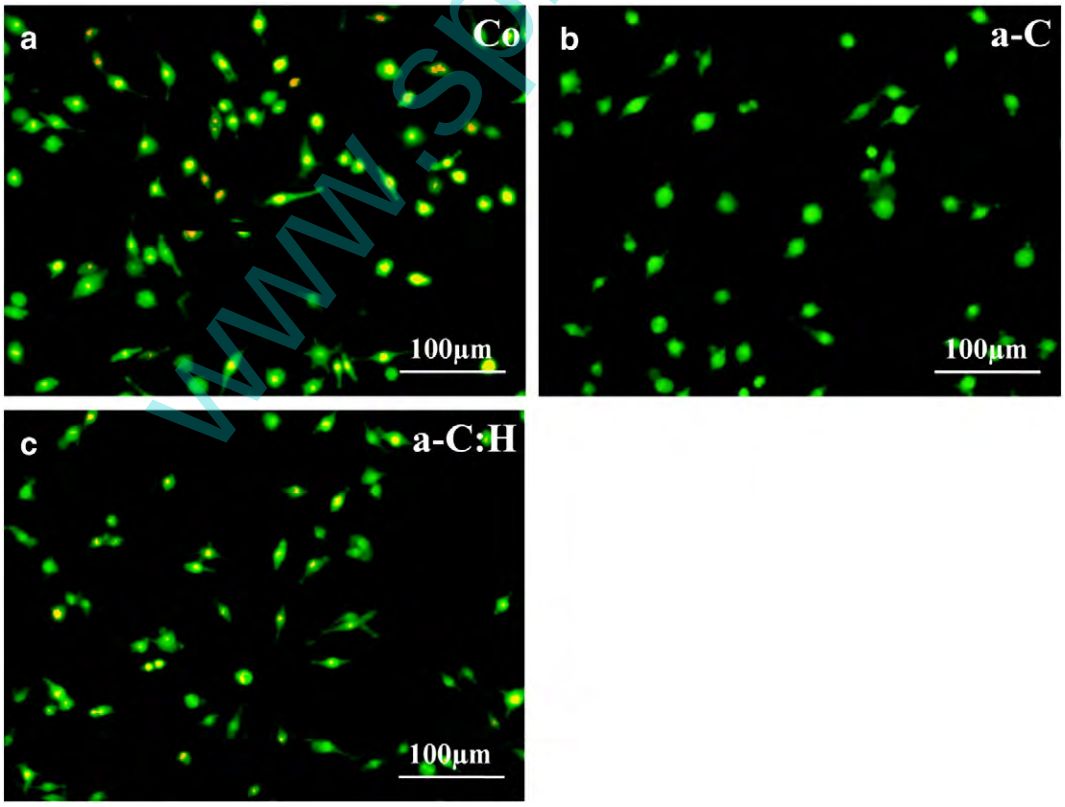

Fig. 3. Death of macrophages cultured on (a) CoCr alloy, (b) a-C films and (c) a-C:H films stained by AO/PI.

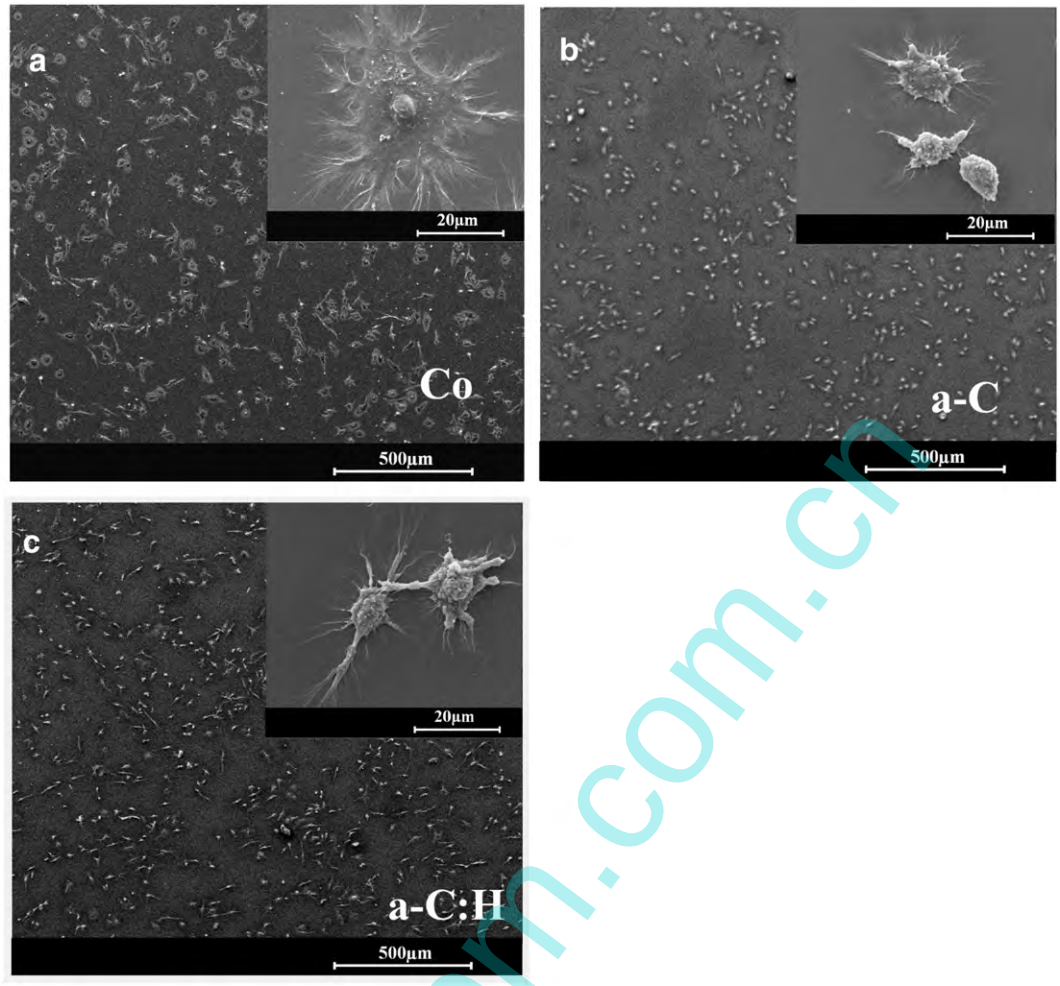

Fig. 4. SEM images of macrophages cultured on (a) Co alloy, (b) a-C and (c) a-C:H for 24 h.

measured by ELISA, and presented in Fig. 5. It shows that macrophages on a-C film release less IL-6 than that on the a-C:H film ($p < 0.05$). The same trend tends to be reproduced also for the TNF-α release (not significant). The a-C films show a lower inflammatory response than a-C:H film.

All results show that both a-C film and a-C:H film induce lower inflammatory reaction than the Co alloy. The a-C film induces less macrophage activation, no macrophage death and lower levels of TNF-α and IL-6 release, indicating a lower inflammatory response to a-C than to a-C:H films.

3.4. Osteoblast cytotoxicity

Cell attachment was characterized by statistic analysis of the number of adherent cells after 2 h incubation. The data are shown in Fig. 6, more osteoblasts adhered on a-C:H film when cells initially contacted the material in 2 h. The viability of osteoblasts cultured on a-C, a-C:H and Co alloy was evaluated by CCK-8. As shown in Fig. 7, osteoblasts cultured on a-C and a-C:H films show better viability than osteoblasts on Co alloy at all three time points of 1 day, 3 days and 6 days. Compared with a-C:H film, the a-C induced higher osteoblasts viability in the 3rd and 6th days.

The morphology of osteoblasts is shown in Fig. 8. Normal individual osteoblasts are polygonal or triangular, with an average size of 10–15 μm in width and 50–80 μm in length. Their good adhesion on the material surface can be characterized by the presence of lamellipodia that strongly adhere to the substrate [11]. It is observed that most of the cells cultured on CoCr alloy (Fig. 8a), a-C film (Fig. 8b) and a-C:H film (Fig. 8c) for 1 day are polygonal and spreading, indicating a normal cell activity. The long and abundant cytoplasmic extensions in multiple directions prove the excellent adhesion behavior of the cells on the surface of the different substrates [17]. Moreover, stack-up cells and bone whirlpool turn up on the CoCr alloy (Fig. 8d), a-C film (Fig. 8e) and a-C:H film (Fig. 8f) after 3 day culture, displaying a trend of osteogenic behavior.

In conclusion, osteoblasts cultured on a-C and a-C:H film show higher viability than that cultured on Co alloy. Compared with a-C:H film, a-C film has less osteoblasts adhesion on the surface in the first 2 h (shown in Fig. 6). But the viability and proliferation ability of the osteoblasts on the a-C film is much higher than that on the a-C:H film in the 3rd and 6th days.

4. Discussion

DLC films are suggested to be applied on MOM artificial joints to reduce the wear of the prosthesis. Since a-C film and a-C:H film show different tribology properties due to the different microstructure and surface properties [16,31,32], differences in cytocompatibility of a-C and a-C:H film should also be considered. What's more, because wear debris of artificial joint may cause osteolysis, aseptic loosening and eventually lead to prosthesis failure [4,6,7], the cytotoxicity of DLC debris is also worth for research [33]. As we all know, DLC film is hard and has excellent wear resistance, so it is difficult to collect wear debris for in vitro evaluation. And DLC films are a group of materials, different bulk material will generate different debris. So it is impossible to collect

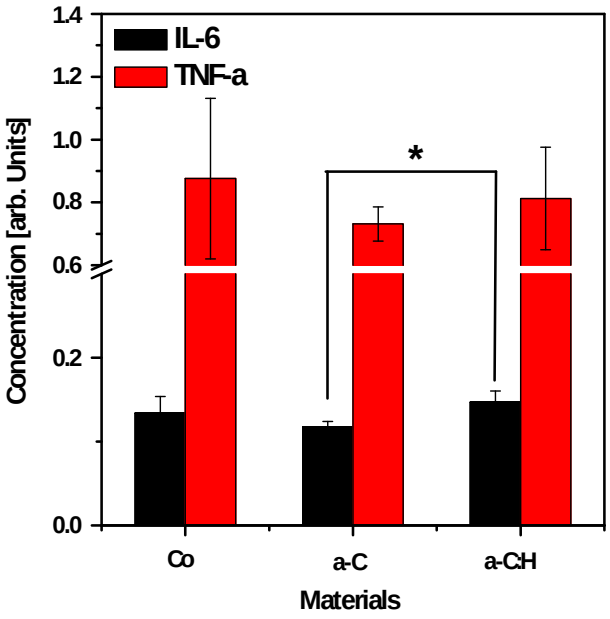

Fig. 5. IL-6 and TNF-α release of Raw 264.7 macrophages after 24 h culture on the various surfaces determined by ELISA. (Data given as mean ± SD, the statistical significance is indicated by $^{*}p < 0.05$, $n = 4$).

debris of all DLC films with different microstructure and surface properties and to study their cytotoxicity. In our strategy, we firstly picked over the DLC films and evaluated inflammatory reaction and osteoblasts cytotocxity of DLC films, looking for more cytocompatible one in this work. After that we will fabricate debris of the more cytocompatible DLC film. Then we will focus on cytocompatibility evaluation of DLC debris.

In this paper, the cytocompatibility of hydrogenated and unhydrogenated carbon film has been studied and the results show that a-C film activates fewer macrophages and induces higher osteoblasts viability than a-C:H film. This is result from different physical/chemical properties of a-C and a-C:H film.

Compared with a-C:H film, a-C film has less osteoblasts adhesion on the surface in the first 2 h (shown in Fig. 6). Surface energy is proven

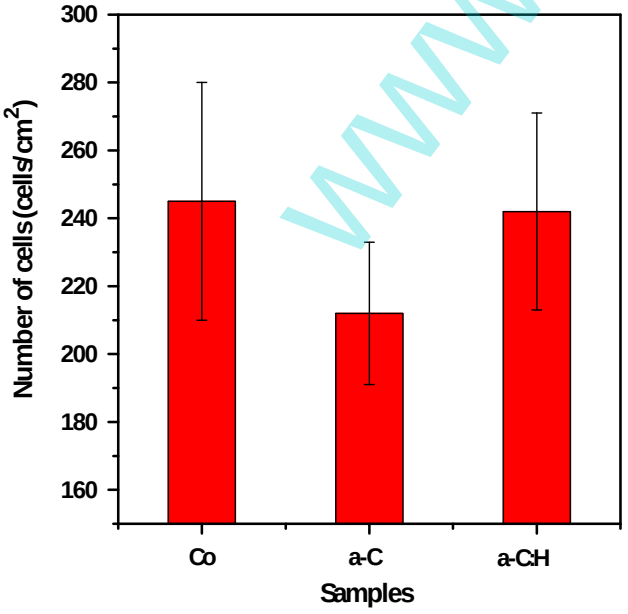

Fig. 6. Number of adherent osteoblasts after 2 h cultivation on the surfaces.

to be an important factor that has effect on cell attachment. It is widely accepted that higher surface energy generally results in better cell adhesion in the beginning when cells attach to a materials surface [13,34]. Comparing with a-C film, a-C:H film has higher surface energy, so more osteoblasts adhere on a-C:H film in the first 2 h (Fig. 6). But the surface energy only influences the cell attachment in the initial period. We can find that osteoblasts on a-C film show higher viability than that cultured on a-C:H film in the 3rd and 6th days of culture (Fig. 7). This may result from different protein adsorption behavior of a-C film and a-C:H film, because protein layer formed at the solid/liquid interface will determine the cell behavior with longer cell culture duration [11,35].

The schematic diagram of adsorbed protein layer and its mediation to osteoblasts growth and proliferation on a-C and a-C:H film is shown in Fig. 9. Compared with a-C:H film, a-C film is more hydrophobic (the water contact angle of a-C:H and a-C is 69.9 ± 3.2 degrees and 87.5 ± 0.3 degrees, respectively), the hydrophobic surface state displays better affinity to proteins [36], so more proteins (BSA and serum protein) adsorbed on a-C film than a-C:H film (Table 2). In this study, a-C film has a large I_D/I_G ratio of 1.99, reflecting the disorder and high graphic content of a-C film, which will generate significant concentrations of unpaired electrons. The unpaired electrons belong to radical-containing groups trapped in the bulk of the surfaces [37], and such groups have high reactivity with amino acid residues to form covalent binding [38,39]. Thus, the a-C film is likely to covalent bind more proteins (Table 2). Covalent binding has been reported to provide a strong bond wherein the function of the attached proteins can be preserved [39–42]. So the proteins on a-C film are stable and bioactive as illustrated in Fig. 9a, which will enhance the osteoblasts spreading and proliferation. Besides, as shown in Fig. 9a, the adsorbed proteins provide many binding sites for growth factors and signaling molecules that promote the process of osteoblasts proliferation, which also result in high viability of osteoblasts on a-C film.

However, for the a-C:H film, no carrier mobility is detected, indicating its low covalent binding capability [37]. Hence, the a-C:H film covalent binds fewer proteins than a-C film (Table 2), and most proteins may be absorbed on a-C:H film through weak interactions like van der waals bond as illustrated in Fig. 9b. The weak bound proteins tend to undergo unfolding and loss of activity [39–42], which may have negative influence on osteoblasts spreading and proliferation. And the weakly bound proteins are susceptible to detach from a-C:H film, which will result in loose contact between osteoblasts and a-C:H film. Moreover, a-C:H film adsorbs fewer proteins than a-C film (Table 2), and there are fewer growth factors and signaling molecules adsorbed on a-C:H film

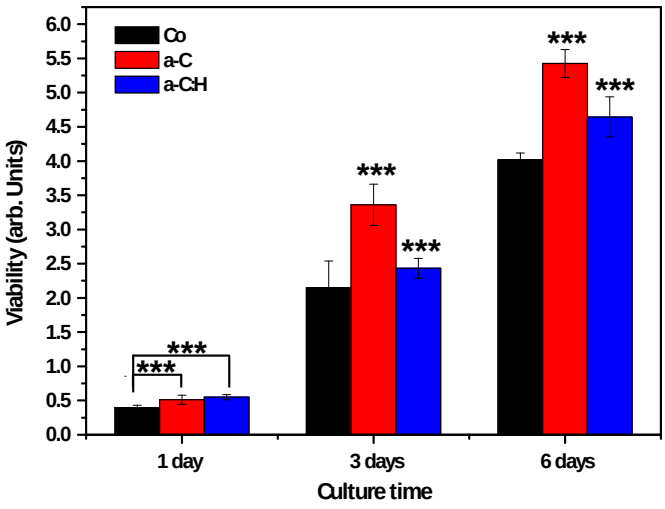

Fig. 7. Viability of mouse osteoblasts on Co alloy, a-C film and a-C:H film after 1 day, 3 days and 6 days, determined by the CCK-8 assay. (Data given as mean ± SD, the statistical significance is indicated by $^{***}p < 0.001$, $n = 6$).

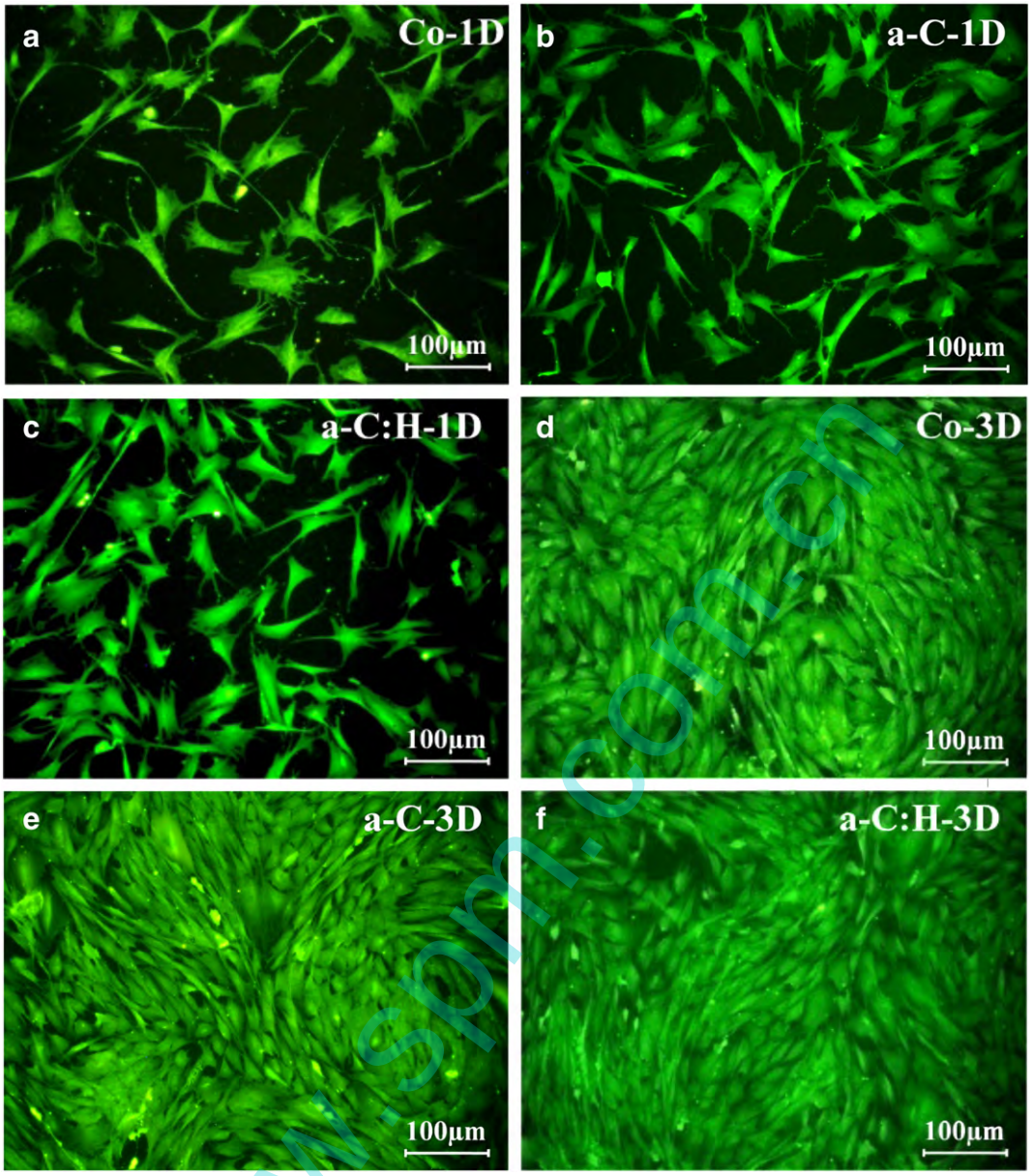

Fig. 8. Fluorescence microscope images of osteoblasts stained by rhodamine 123 on (a) Co alloy, (b) a-C, and (c) a-C:H for 1 day; (d) Co alloy, (e) a-C, and (f) a-C:H for 3 days.

than a-C film, so osteoblasts cultured on a-C:H film show relatively lower viability than that cultured on a-C film.

Apart from the osteoblasts behavior, the different reaction of macrophages cultured on a-C and a-C:H film is also mediated by the protein layer. In this study, a-C film activates fewer macrophages than a-C:H film (Fig. 4). It is known that when macrophages are cultured on solid materials, the denatured proteins on the surface will induce the "frustrated phagocytosis" as macrophages attempt [43]. As we discussed above, the proteins adsorbed on a-C film are mostly bioactive because of covalent binding, so most of the macrophages on a-C film will not be activated. But some proteins adsorbed on a-C:H film are likely to be denatured because of weak interaction, thus more macrophages on a-C:H film are activated.

5. Conclusion

In this paper, the cytocompatibility of a-C and a-C:H film was evaluated, and the relationship of the physical/chemical properties and cell behavior of DLC films was studied. The a-C film shows superior cytocompatibility to osteoblasts and less inflammatory response than a-C:H film. Compared with a-C:H film, a-C film is more hydrophobic and contains more unpaired electrons. The hydrophobic surface state of a-C film displays better affinity to proteins. The unpaired electrons in a-C film induce covalent binding between proteins and a-C film, providing a strong bond wherein the function of the attached proteins can be preserved. However, some of the adsorbed proteins on a-C:H film tend to be denatured. The superior adsorption and bioactivity of the adhesive proteins on a-C film finally result in its better cytocompatibility than a-C:H film.

Acknowledgment

The authors would like to thank Dr. Y.M. Liu and Dr. F. Shi for cell assistance and thank Dr. J.A.Li, Dr. P.K.Qi and Dr. Y.Yang for their help in discussing this paper. This work was supported by Natural Science Foundation of China (81271953).

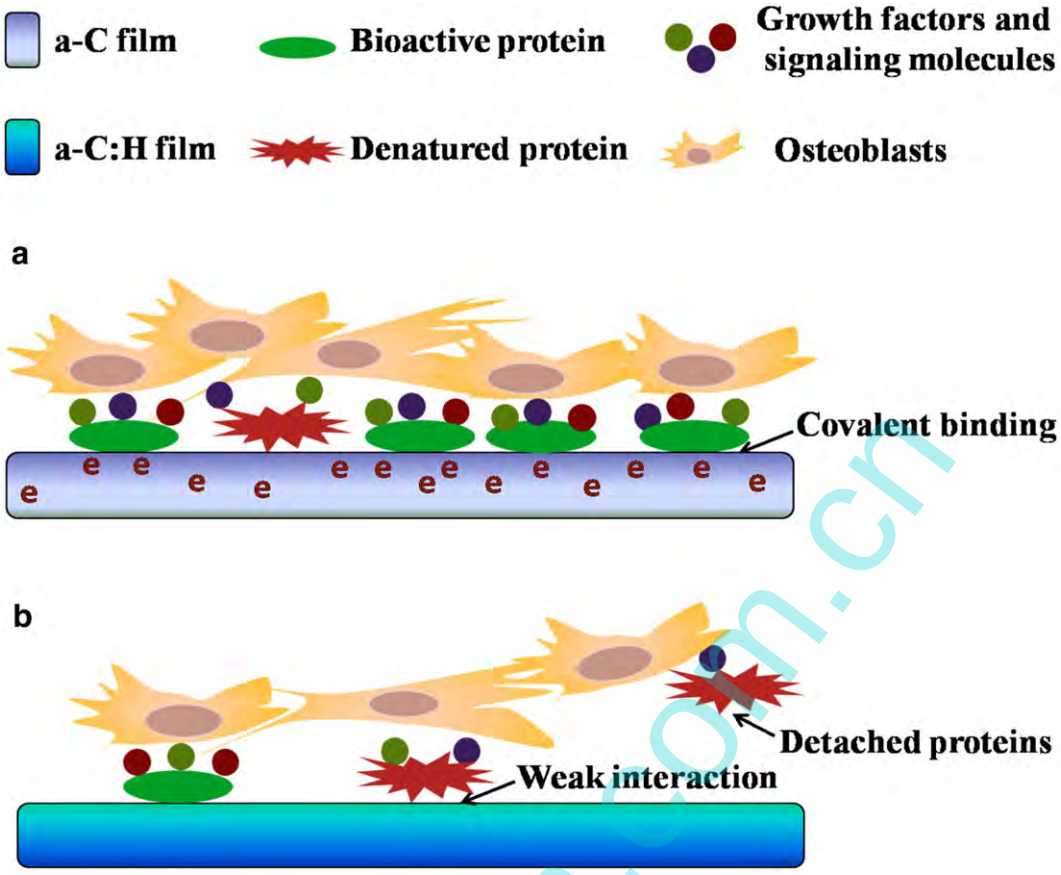

Fig. 9. Schematic diagram of adsorbed protein layer and mediation of adsorbed proteins to osteoblasts adhesion and growth on (a) a-C film and (b) a-C:H film.

References

[1] Pascal-André Vendittoli, Traian Amzica, Lain G. Roy, Daniel Lusignan, Julien Girard, Martin Lavigne, J. Arthroplast. 26 (2) (2011) 282–288.
[2] Ryan G. Molli, Adolph V. Lombardi, Keith R. Berend, Joanne B. Adams, Michael A. Sneller, J. Arthroplast. 26 (6) (2011) 8–13.
[3] I. Papageorgiou, C. Brown, R. Schins, S. Singh, R. Newson, S. Davis, J. Fisher, E. Ingham, C.P. Case, Biomaterials 28 (2007) 2946–2958.
[4] Arihiko Kanaji, Marco S. Caicedo, Amarjit S. Virdi, D. Rick Sumner, Nadim J. Hallab, Kotaro Sena, Bone 45 (2009) 528–533.
[5] Martin Figgitt, Roger Newson, Ian J. Leslie, John Fisher, Eileen Ingham, Charles P. Case, Mutat. Res. 688 (2010) 53–61.
[6] Daniel Howcroft, Marcus Head, Niall Steele, Curr. Orthop. 22 (2008) 177–184.
[7] Geoffrey Dearnaley, James H. Arps, Surf. Coat. Technol. 200 (2005) 2518–2524.
[8] Veli-Matti Tiainen, Diam. Relat. Mater. 10 (2001) 153–160.
[9] A. Anttila, R. Lappalainen, H. Heinonen, S. Santavirta, Y.T. Konttinen, New Diam. Front. Carbon Technol. 9 (1999) 283–288.
[10] Huaiyu Wang, Ming Xu, Wei Zhang, Dixon T.K. Kwok, Jiang Jiang, Zhengwei Wu, Paul K. Chu, Biomaterials 31 (2010) 8181–8187.
[11] Feng Chai, Nicolas Mathis, Nicolas Blanchemain, Cathy Meunier, Hartmut F. Hildebrand, Acta Biomater. 4 (2008) 1369–1381.
[12] E. Salgueiredo, M. Vila, M.A. Silva, M.A. Lopes, J.D. Santos, F.M. Costa, R.F. Silva, P.S. Gomes, M.H. Fernandes, Diam. Relat. Mater. 17 (2008) 878–881.
[13] Wen J. Ma, Andrew J. Ruys, Rebecca S. Mason, Phil J. Martin, Avi Bendavid, Zongwen Liu, Mihail Ionescu, Hala Zreiqat, Biomaterials 28 (2007) 1620–1628.
[14] M. Ball, A. O'Brien, F. Dolan, G. Abbas, J.A. McLaughlin, J. Biomed. Mater. Res. 70A (2004) 380–390.
[15] M. Grischke, A. Hieke*, F. Morgenweck, H. Dimigen, Diam. Relat. Mater. 7 (1998) 454–458.
[16] Xingbin Yan, Xu. Tao, Gang Chen, Shengrong Yang, Huiwen Liu, Appl. Surf. Sci. 236 (2004) 328–335.
[17] C. Meunier, Y. Stauffer, A. Daglar, F. Chai, S. Mikhailov, H.F. Hildebrand, Surf. Coat. Technol. 200 (2006) 6346–6349.
[18] Hengjun Liu, Yongxiang Leng, Jinglong Tang, Shuo Wang, Dong Xie, Hong Sun, Nan Huang, Surf. Coat. Technol. 206 (2012) 4907–4914.
[19] X.R. Deng, Y.X. Leng, X. Dong, H. Sun, Nan Huang, Surf. Coat. Technol. 206 (2011) 1007–1010.
[20] T. Futami, N. Fujii, H. Ohnishi, N. Taguchi, H. Kusakari, H. Ohshima, et al., J. Periodontol. 71 (2000) 287–298.
[21] M. Leite, M. Quina-Costa, P.S. Leite, et al., Anal. Cell. Pathol. 19 (3–4) (1999) 139–151.
[22] R.I. Freshney, Culture of animal cells: a manual of basic technique, John Wiley-Liss, New York, 2000.
[23] Y.F. Lu, S.M. Huang, Z. Sun, J. Appl. Phys. 87 (2000) 945–951.
[24] N.W. Khun, E. Liu, G.C. Yang, W.G. Ma, S.P. Jiang, J. Appl. Phys. 106 (2009) 013506-1–013506-9.
[25] H. Tapper, J. Leukoc. Biol. 59 (1996) 613–622.
[26] E. Ingham, J. Fisher, Biomaterials 26 (2005) 1271–1286.
[27] Guicai Li, Ping Yang, Xiang Guo, Nan Huang, Ru Shen, Cytokine 56 (2011) 208–217.
[28] J. Julow, M. Ishii, T. Iwabuchi, Acta Neurochir. 50 (1979) 273–280.
[29] R.J. Schutte, A.P. Amon, W.M. Reichert, J. Biomed. Mater. Res. A 88 (2009) 128–139.
[30] A. Sabokbar, O. Kudo, N.A. Athanasou, J. Orthop. Res. 21 (2003) 73–80.
[31] Kenji Yamamoto, Katsuhiro Matsukado, Tribol. Int. 39 (2006) 1609–1614.
[32] Guojia Ma, Shuili Gong, Guoqiang Lin, Lin Zhang, Gang Sun, Appl. Surf. Sci. 258 (2012) 3045–3050.
[33] Arie Bruinink, Anouk Schroeder, Gilbert Francz, Roland Hauert, Biomaterials 26 (2005) 3487–3494.
[34] G. Altankov, T. Groth, J. Mater. Sci. Mater. Med. 5 (1994) 732–737.
[35] Cameron J. Wilson, Richard E. Clegg, David I. Leavesley, M.A.R.K.J. Pearcy, Tissue Eng. 11 (2005) 1–18.
[36] A. Michiardi, C. Aparicio, B.D. Ratner, J.A. Planell, J. Gil, Biomaterials 28 (2007) 586–594.
[37] Yongbai Yin, Keith Fisher, Neil J. Nosworthy, Daniel Bax, Ron J. Clarke, David R. McKenzie, Marcela M.M. Bilek, Thin Solid Films 520 (2012) 3021–3025.
[38] Yongbai Yin, Marcela M.M. Bilek, David R. McKenzie, Plasma Process. Polym. 7 (2010) 708–714.
[39] Marcela M.M. Bilek, Daniel V. Bax, Alexey Kondyurin, Yongbai Yin, Neil J. Nosworthy, Keith Fisher, Anna Waterhouse, Anthony S. Weiss, Cristobal G. dos Remedios, David R. McKenzie, PNAS 108 (2011) 14405–14410.
[40] Anna Waterhouse, Steven G. Wise, Yongbai Yin, Buchu Wu, Barbara James, Hala Zreiqat, David R. McKenzie, Shisan Bao, Anthony S. Weiss, Martin K.C. Ng, Marcela M.M. Bilek, Biomaterials 33 (2012) 7984–7992.
[41] Yongbai Yin, Steven G. Wise, Neil J. Nosworthy, Anna Waterhouse, Daniel V. Bax, Hani Youssef, Michael J. Byrome, Marcela M.M. Bilek, David R. McKenzie, Anthony S. Weiss, Martin K.C. Ng, Biomaterials 30 (2009) 1675–1681.
[42] Marcela M. Bilek, David R. McKenzie, Biophys. Rev. 2 (2010) 55–65.
[43] P. Thomsen, C. Gretzer, Curr. Opin. Solid State Mater. Sci. 5 (2001) 163–176.